



**University of  
Zurich**<sup>UZH</sup>

**Zurich Open Repository and  
Archive**

University of Zurich  
University Library  
Strickhofstrasse 39  
CH-8057 Zurich  
[www.zora.uzh.ch](http://www.zora.uzh.ch)

---

Year: 2010

---

## **First evidence of a bipartite medial cuneiform in the hominin fossil record: a case report from the Early Pleistocene site of Dmanisi**

Jashashvili, T ; Ponce de León, M S ; Lordkipanidze, D ; Zollikofer, C P E

**Abstract:** A medial cuneiform exhibiting complete bipartition was discovered at the Early Pleistocene site of Dmanisi, Georgia. The specimen is the oldest known instance of this anatomical variant in the hominin fossil record. Here we compare developmental variation of the medial cuneiform in fossil hominins, extant humans and great apes, and discuss potential implications of bipartition for hominin foot phylogeny and function. Complete bipartition is rare among modern humans (< 1%); incomplete bipartition was found in 2 of 200 examined great ape specimens and also appears in the form of a divided distal articular surface in the Stw573c *Australopithecus africanus* specimen. Although various developmental pathways lead to medial cuneiform bipartition, it appears that the bipartite bone does not deviate significantly from normal overall morphology. Together, these data indicate that bipartition represents a phylogenetically old developmental variant of the medial cuneiform, which does not, however, affect the species-specific morphology and function of this bone.

DOI: <https://doi.org/10.1111/j.1469-7580.2010.01236.x>

Posted at the Zurich Open Repository and Archive, University of Zurich

ZORA URL: <https://doi.org/10.5167/uzh-44327>

Journal Article

Originally published at:

Jashashvili, T; Ponce de León, M S; Lordkipanidze, D; Zollikofer, C P E (2010). First evidence of a bipartite medial cuneiform in the hominin fossil record: a case report from the Early Pleistocene site of Dmanisi. *Journal of Anatomy*, 216(6):705-716.

DOI: <https://doi.org/10.1111/j.1469-7580.2010.01236.x>

# First evidence of a bipartite medial cuneiform in the hominin fossil record: a case report from the Early Pleistocene site of Dmanisi

Tea Jashashvili,<sup>1,2</sup> Marcia S. Ponce de León,<sup>1</sup> David Lordkipanidze<sup>2</sup> and Christoph P. E. Zollikofer<sup>1</sup>

<sup>1</sup>Anthropological Institute and Museum, University of Zurich, Zurich, Switzerland

<sup>2</sup>Department of Geology and Paleontology, Georgian National Museum, Tbilisi, Georgia

## Abstract

A medial cuneiform exhibiting complete bipartition was discovered at the Early Pleistocene site of Dmanisi, Georgia. The specimen is the oldest known instance of this anatomical variant in the hominin fossil record. Here we compare developmental variation of the medial cuneiform in fossil hominins, extant humans and great apes, and discuss potential implications of bipartition for hominin foot phylogeny and function. Complete bipartition is rare among modern humans (< 1%); incomplete bipartition was found in 2 of 200 examined great ape specimens and also appears in the form of a divided distal articular surface in the Stw573c *Australopithecus africanus* specimen. Although various developmental pathways lead to medial cuneiform bipartition, it appears that the bipartite bone does not deviate significantly from normal overall morphology. Together, these data indicate that bipartition represents a phylogenetically old developmental variant of the medial cuneiform, which does not, however, affect the species-specific morphology and function of this bone.

**Key words** Dmanisi; morphogenesis; *os cuneiforme mediale bipartitum*; tarsal bones.

## Introduction

The Early Pleistocene site of Dmanisi, Georgia provides a rich assemblage of hominin fossils dated to approximately 1.77 Ma (Vekua et al. 2002; Lordkipanidze et al. 2005, 2006, 2007). During the 2002 excavation season, two nearly complete hominin bones (D4111 and D4112) were discovered in the Block 2 excavation area (square N64/61, layer B1x). Upon subsequent examination, the bones were found to articulate into a single right medial cuneiform. Medial cuneiform bipartition in Dmanisi is similar to what has been described in earlier studies of modern human samples (Barclay, 1932; Barlow, 1942; Kjellström, 2004). The two portions of the Dmanisi bipartite medial cuneiform are referred to subsequently as D4111a/b. D4111a/b is associated anatomically with the first metatarsal D3442 (Lordkipanidze et al. 2007). According to modern human developmental standards, these elements represent an adult individual (the D3442 metatarsal has a fully fused proximal epiphysis; in modern humans, metatarsal I fusion ages are 13–15 years

for females and 16–18 years for males, and the medial cuneiform reaches adult morphology by about 6 years of age; Scheuer & Black, 2000).

Bipartition of different human skeletal elements is a relatively frequent subject of comparative anatomical studies. By definition, bipartition means the division of one whole element into two separately-formed parts. Bipartition of bones does not always necessarily equate to two separate, but equal, segments. Bipartition of several carpal and tarsal bones has been described in humans, such as the lunate (Gruber, 1883, 1884; Eggimann, 1951; Schmitt & Schmitt, 1983), scaphoid (Randelli, 1961; Richards et al. 1987) and navicular (Volk, 1937; Zimmer, 1938; Hubner, 1953; Mau, 1960; Wiley & Brown, 1981; Shawdon et al. 1995). The most frequently observed example of a bipartite condition amongst tarsal bones, however, is the medial cuneiform (*os cuneiforme mediale bipartitum*), first described by Smith (1866) (see Table 1). Bipartition of the medial cuneiform typically results in the bone being divided into upper (dorsal) and lower (plantar) elements. Both of the bipartite elements collectively represent the same structure as appears in non-bipartite medial cuneiforms (Fig. 1).

In the present case study, we provide an anatomical description of a bipartite medial cuneiform from Dmanisi, which is the earliest instance of this anatomical condition that has been reported in the hominin fossil record. We perform morphometric comparisons with five modern human

## Correspondence

Dr Tea Jashashvili, Anthropological Institute and Museum, University of Zurich, Winterthurerstrasse 190, CH-8057 Zurich, Switzerland.  
T: +41446355441; F: +41446356886; E: tjashashvili@aim.uzh.ch

Accepted for publication 10 March 2010

**Table 1** Case list of modern human bipartite medial cuneiforms.

Author	Categories of bipartition, number of cases and provenance	Form of proximal articular surface of first metatarsal
Jones (1864) as mentioned by Barlow (1942)	Unilateral complete (1)	–
Smith (1866)	Bilateral complete (1), dissection material	Two distinct articular facets
Turner (1869)	Partial (4), osteological material	–
Stieda (1869) in Barlow (1942)	Complete (1)	–
Ledentu (1869) as mentioned by Barlow (1942)	Unilateral complete (1), archaeological material	–
Friedlowsky (1870)	Complete (2)	–
Gruber (1877)	Unilateral complete (1)	Two distinct articular facets
	Bilateral complete (4), unilateral complete (6)	Two distinct articular facets
	Partial (7)	
	Total sample: 2584	
Hartman & Mordret (1889)	Complete (2)	Two distinct articular facets
	Incomplete (20), different stages of grooving or furrowing	
	Total sample: 100	
Pfizzner (1896)	Complete (4)	Two distinct articular facets
	Incomplete (6)	
	Total sample: 450	
Volkov (1904)	Complete (1), Merovingian	–
Holtby (1916) in Barlow (1942)	Bilateral complete (1)	Two distinct articular facets
Virchow (1922)	Incomplete right medial cuneiform (1)	–
Willich (1925)	Bilateral complete (1)	Two distinct articular facets
Barclay (1932)	Bilateral complete (1), Clinical	–
Böker & Müller (1936)	Complete (1)	–
Barlow (1942)	Complete (1)	–
Marti (1947)	Complete (3)	–
Weber (1956)	Complete (1)	–
Dellacorte et al. (1992)	Bilateral complete (1), clinical	–
O'Neal et al. (1995)	Bilateral complete (1), clinical	–
Sener (1999)	Bilateral complete (1), clinical (Rubinstein–Taybi syndrome)	–
Azurza & Sakellariou (2001)	Bilateral complete (1), clinical	–
Chiodo et al. (2002)	Complete (1), clinical	–
Kjellström (2004)	Bilateral complete (1), specimen Sk24 bilateral incomplete (1), specimen Sk28	–
Bismil et al. (2005)	Complete (1), clinical	–
Fulwadhva & Parker (2007)	Complete (1), clinical	–
Elias et al. (2008)	Complete (4), clinical	–

–, no information.

populations, including bipartite samples from historical grave burials dated to the 9<sup>th</sup>–11<sup>th</sup> centuries in Sigtuna, Sweden (Kjellström, 2004). We also compare the morphology of the Dmanisi medial cuneiform and its associated metatarsal with similar elements in other fossil hominins, focusing on the morphology of the joint between the medial cuneiform and metatarsal I. Using this evidence, we ask whether bipartition of the medial cuneiform may be functionally advantageous during the evolution of hominin locomotion or whether it represents anatomical variation arising from variation in developmental pathways.

## Materials and methods

Data on the incidence and morphological variants of medial cuneiform bipartition in modern human populations and fossil hominins were compiled from the literature. Comparative data on frequencies amongst hominoids were collected from a sample ( $n = 200$ ) comprised of *Pan troglodytes*, *P. paniscus*, *Gorilla gorilla* and *Pongo pygmaeus* specimens from the Royal Museum of Central Africa (RMCA), Tervuren and the Anthropological Institute and Museum (AIM), University of Zurich. Data for non-hominoid primate species were compiled from the literature.

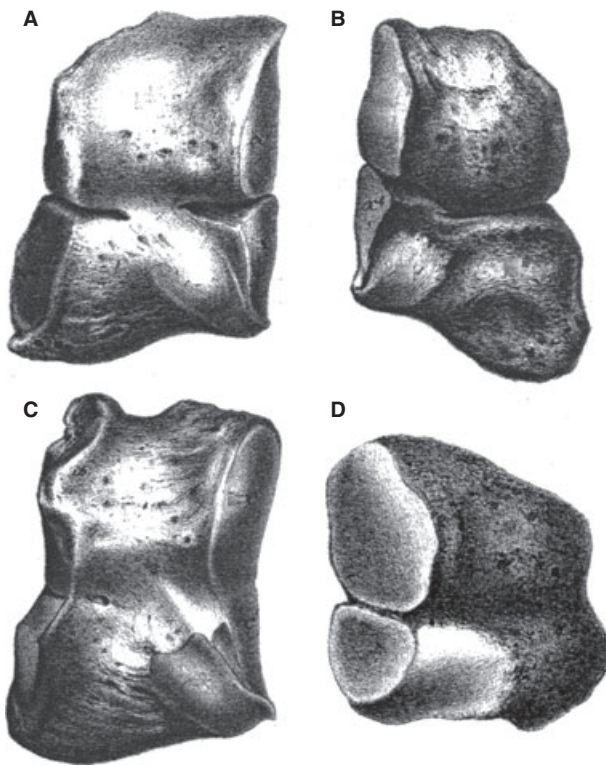


**Fig. 1** Degrees of bipartition in the medial cuneiform. (A,B) Complete bipartition; (C) Incomplete bipartition; (D) division of the distal articular surface. From Gruber (1877).

The modern human sample of medial cuneiforms used for morphometric comparisons includes data from five populations: recent African-Americans ( $n = 20$ ); archaeological specimens from St Sisinius cemetery (11<sup>th</sup>–12<sup>th</sup> century), Laas, South Tyrol ( $n = 20$ ) (A. H. Schultz Collection, Anthropological Institute, University of Zurich); archaeological specimens from Taforalt, Morocco (ca. 12 000 BP) ( $n = 26$ ) (Mariotti et al. 2009) and Afalou bou-Rhumel, Algeria (10 500–8500 BP) ( $n = 12$ ) (Mirazón Lahr & Arensburg, 1995) (Institut de Paléontologie Humaine, Paris); and a sample of bipartite medial cuneiforms from a 9<sup>th</sup>–11<sup>th</sup> century mass grave in Sigtuna, Sweden ( $n = 6$ ) (Kjellström, 2004).

Linear dimensions of normal and bipartite medial cuneiforms were measured to quantify the overall size and articular dimensions of the bone, following the measurement definitions of Martin & Saller (1957) and Trinkaus (1983) (see Fig. 2). Superior length (SL) is the distance between the most projecting point of the superior (dorsal) edge of the proximal joint area and the corresponding point of the distal joint area of the bone. Middle length (ML) is the distance between the most projecting point of the middle edge of the proximal articular area and the corresponding point of the distal articular area of the bone. Inferior length (IL) is the distance between the most projecting points of the lower (plantar) edge of the proximal articular area and the corresponding point of the distal articular area of the bone. Proximal height (PH) is the distance between the highest (dorsal) point of the superior edge and the deepest (plantar) point of the base of the bone at the proximal end (i.e. not at the edges of the articular area). Proximal articular height (PAH) is the distance between the highest (dorsal) and the deepest

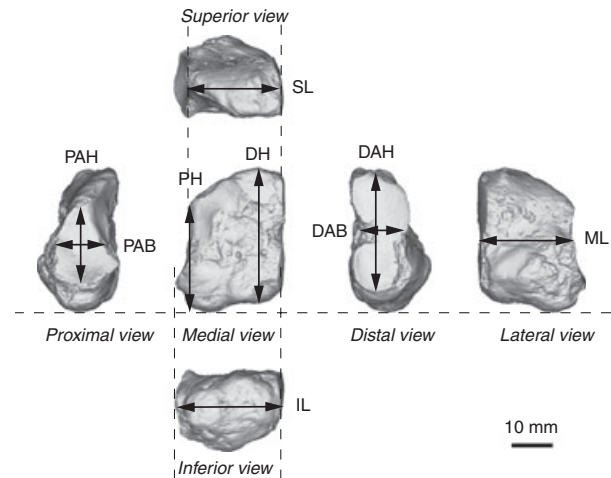


**Fig. 2** Definition of measurements (modern human right medial cuneiform with division of the articular surface) (micro-computed tomography-based data of an archaeological specimen from Vaihingen an der Enz, Germany, specimen no. 190-10). SL, superior length; ML, middle length; IL, inferior length; PH, proximal height; PAH, proximal articular height; PAB, proximal articular breadth; DH, distal height; DAH, distal articular height; DAB, distal articular breadth.

(plantar) points of the proximal joint area. Proximal articular breadth (PAB) (Trinkaus, 1983) is the distance between the medial and lateral points at the middle of the proximal joint area, perpendicular to PAH. Distal height is the distance between the highest (dorsal) point of the superior edge and the deepest (plantar) point of the base of the bone at the distal end. Distal articular height (DAH) is the distance between the highest (dorsal) and the deepest (plantar) points of the distal joint area. Distal articular breadth (DAB) (Trinkaus, 1983) is the distance between the medial and the lateral point at the middle of the distal joint area, perpendicular to DAH. All measurements were taken using sliding calipers with a precision of 0.1 mm. Means, SDs and ranges are presented in Table 2. Using these measurements, the following additional variables were calculated in order to estimate articular surface areas: proximal articular area (PAH\*PAB) and distal articular area (DAH\*DAB).

## Results

### Review of reported cases of bipartite medial cuneiforms

All reported cases of a bipartite medial cuneiform in modern humans can be assigned to one of three morphological categories (Fig. 1).

**1 Complete bipartition**, in which the medial cuneiform is divided into separate upper (dorsal) and lower (plantar) elements (Fig. 1A,B).

**2 Incomplete bipartition**, in which the two segments are partially fused, with a well-marked proximo-distal cleft on the medial and lateral surfaces demarcating dorsal and plantar segments (Fig. 1C).

**Table 2** Linear dimensions of medial cuneiforms (mm).

Variables	Afro-American (N = 19)	Laas (N = 20)	Taforalt (N = 26)	Afalou (N = 12)	Sigtuna (N = 6)	Dmanisi D4111a/b
SL	24.87 ± 1.45 22.10–27.30	23.71 ± 2.26 19.90–28.90	24.94 ± 1.53 22.24–27.58	24.87 ± 1.70 22.24–27.77	24.62 ± 0.82 23.40–25.60	16.40
ML	23.80 ± 1.39 21.50–25.90	21.91 ± 1.58 19.20–24.60	24.45 ± 1.47 21.61–27.33	24.17 ± 1.42 21.77–26.91	22.50 ± 1.36 21.00–24.20	16.60
IL	27.51 ± 1.67 24.60–30.30	25.39 ± 2.18 22.40–29.80	26.57 ± 1.46 23.41–28.97	26.57 ± 2.69 22.30–30.66	27.38 ± 1.10 26.40–29.20	20.10
PH	28.68 ± 1.77 25.80–31.40	26.00 ± 2.14 22.90–29.70	24.38 ± 2.21 21.19–29.71	24.17 ± 2.78 19.10–28.77	29.35 ± 2.12 26.20–32.40	17.50
PAH	23.11 ± 1.56 20.10–25.50	21.32 ± 1.95 16.90–24.10	20.29 ± 2.10 16.47–24.70	20.80 ± 1.91 18.14–23.70	25.47 ± 3.47 21.30–30.30	13.10
PAB	15.99 ± 1.36 12.90–17.90	15.86 ± 1.65 13.20–18.10	15.81 ± 1.36 13.07–18.03	15.93 ± 1.39 13.41–17.59	16.58 ± 0.75 15.90–17.90	13.50
DH	33.84 ± 2.51 30.05–38.50	30.96 ± 2.29 27.70–34.90	32.80 ± 1.94 29.43–35.90	33.18 ± 2.40 27.70–35.86	34.08 ± 1.51 32.10–35.90	28.80
DAH	30.88 ± 2.07 27.50–34.40	28.17 ± 1.85 25.50–32.40	29.38 ± 1.74 25.55–31.83	29.50 ± 2.30 25.29–32.99	30.45 ± 1.20 28.70–31.90	26.40
DAB	13.14 ± 1.20 11.20–15.50	13.03 ± 2.15 9.70–17.40	12.63 ± 1.51 10.17–16.14	13.64 ± 1.18 12.02–15.86	13.80 ± 0.88 12.30–14.80	12.50

SL, superior length; ML, middle length; IL, inferior length; PH, proximal height; PAH, proximal articular height; PAB, proximal articular breadth; DH, distal height; DAH, distal articular height; DAB, distal articular breadth.

Data represent mean ± SD (first row), and range (second row).

**3 Division of the distal articular surface (Fig. 1D).** The latter variant seems to be the most commonly observed (Barlow, 1942).

Bipartition can affect one or both feet of an individual, which is referred to here as unilateral and bilateral cases, respectively. Table 1 provides a list of reported cases of each category, demonstrating that bipartition is relatively rare. In the largest sample examined so far, an incidence of 0.27 and 0.39% was reported for complete and partial bipartitions, respectively (Gruber, 1877). A high frequency of bipartition has been encountered in populations of low genetic diversity, such as bilateral bipartition to various degrees in three individuals from a burial site in Sigtuna, Sweden (Kjellström, 2004). This indicates a heritable component of the trait (Gruber, 1884; Pfitzner, 1896; Barlow, 1942; Azurza & Sakellariou, 2001; Kjellström, 2004). Although a majority of reports of bipartite medial cuneiforms come from archaeological, osteological or dissection material, the wide use of magnetic resonance imaging and computed tomography in clinical diagnostics of midfoot trauma and pathology has yielded a growing number of cases as incidental clinical findings.<sup>1</sup>

In the bipartite medial cuneiform, an extra-articular joint divides the bone into plantar and dorsal segments.

The size relationship between these elements is variable and appears to be case-specific. Most commonly, there are relatively large plantar and relatively small dorsal portions. Some authors describe the synovial joint as plane-like, similar to joints between other tarsal bones that permit gliding movements (Barlow, 1942). Others propose a cartilaginous synchondrosis (Azurza & Sakellariou, 2001), where the hyaline cartilage (a relic of the embryonic cartilage matrix of the skeleton) creates an immobile synarthrosis joint. In either case, the volume of a bipartite medial cuneiform is slightly larger than that of a typical non-bipartite medial cuneiform. Muscles attaching to a bipartite medial cuneiform are only received by the plantar segment. A slip of the tendons of *tibialis posterior* and *peroneus longus* typically attaches to the plantar surface, whereas the *tibialis anterior* tendon typically attaches to the medial surface of the plantar segment. No muscles are attached to the lateral area of the dorsal segment but instead there is an attachment of an interosseous ligament. Proximally on the medial surface, there is an attachment for a dorsal cuneonavicular ligament, whereas distally there is an attachment for the ligaments of the medial tarsometatarsal joint. Compared with a non-bipartite medial cuneiform, all three categories of the bipartite condition have split articular facets for the first metatarsal and, in some cases, split facets on the navicular and second medial cuneiform (Barlow, 1942).

Descriptions of first metatarsals associated with bipartite medial cuneiforms (all categories) report expansion of the

<sup>1</sup>In all of these cases, medial cuneiform bipartition is asymptomatic and not related to the diagnosed disorder (Dellacorte et al. 1992; Azurza and Sakellariou, 2001; Bismil et al. 2005; Elias et al. 2008).



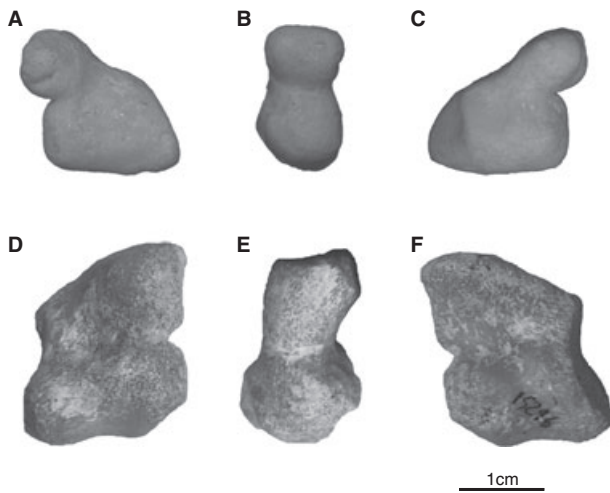


**Fig. 3** Right *Pongo pygmaeus* (AIM10141) medial cuneiform (incomplete bipartition): medial (A), distal (B) and lateral (C) views. Left *Pan paniscus* (RMCA15296) medial cuneiform (incomplete bipartition): medial (D), distal (E) and lateral (F) views.

dorso-plantar diameter and division of the proximal articular surface into two facets separated by a ridge. The upper facet usually is concave, articulating with the anterior facet of the dorsal segment of the bipartite medial cuneiform, whereas the plantar facet usually is slightly convex, articulating with the plantar cuneiform segment (Table 1).

#### Review of reported cases of bipartite medial cuneiforms in non-human primates

Bipartition was observed in two of 200 hominoid specimens. One instance of bipartition was observed in a 6-year-old *Pongo pygmaeus abelii* (Zurich collection id: AIM10141; Fig. 3A–C), whereas the other instance was observed in an adult *P. paniscus* (Tevuren collection id: RMCA15296; Fig. 3D–F). Both of these individuals were classified as incomplete (category 2) bipartition, where a well-marked proximo-distal cleft on the medial and lateral surfaces divides the bone into two regions, dorsal and plantar. These are the first cases of bipartition reported in non-human primates.

#### Review of medial cuneiforms in Plio-Pleistocene hominin fossils

Several medial cuneiforms have been described in the hominin Plio-Pleistocene fossil record: a left, complete one, possibly the earliest available *Australopithecus africanus* specimen (Stw573c) (Clarke & Tobias, 1995); a right, adult *Australopithecus afarensis* specimen (AL333-28) conserving the plantar two-thirds of the element (Latimer et al. 1982); a left, fragmentary specimen attributed to either *Paranthropus robustus* or *Homo cf. erectus* (SKX31117)

(Susman, 1989)<sup>2</sup>; and a left, complete *H. habilis* specimen (OH8e) (Day & Napier, 1964). Medial cuneiforms have also been reported for *H. floresiensis* (Jungers et al. 2009) and *Ardipithecus ramidus* (Lovejoy et al. 2009) but detailed descriptions of their morphology are not yet available.

In initial studies of the Stw573c medial cuneiform (Clarke & Tobias, 1995; Deloison, 2004), the distal articular facet was described as extending onto the medial surface and having a 'less square-shaped' configuration. Such morphology resembles *Pan* (Deloison, 2004). The distal facet of Stw573c is markedly convex. The L-shaped facet for the intermediate cuneiform resembles the condition in modern humans. A recent quantitative analysis (McHenry & Jones, 2006), however, demonstrated that the distal articular facet does not extend onto the medial surface and that the medial cuneiform-metatarsal facet is human-like. A photograph of the distal aspect of this specimen (Deloison, 2004) suggests the presence of two separate distal facets instead of one. Therefore, it is likely that the Stw573c medial cuneiform has a divided distal articular surface (category 3), whereas the proximal surface has a single, undivided facet. In AL333-28, the preserved two-thirds of the distal articulation show a convex facet with a distinct longitudinal-dorso-plantar ridge (Latimer et al. 1982), similar to what has been described in Stw573c. Re-examination of this surface shows no signs of bipartition. Rather, the apparent ridges are due to partial erosion of the articular surface (Tim White, Department of Integrative Biology, University of California, Berkeley, and Berhane Asfaw, Rift Valley Research Service, Addis Ababa, pers. comm.)

The OH8e and SKX31117 medial cuneiforms are different from those of the two australopithecine specimens, primarily in that the former two have a less convex distal articular surface (Day & Napier, 1964; Susman, 1989).

The first metatarsal (Stw573d), which is associated with the Stw573c medial cuneiform, has a slightly concave proximal articular surface divided into upper and lower facets by a transverse ridge (Latimer et al. 1982; Clarke & Tobias, 1995). A first left metatarsal AL333-54, which was found in the same archaeological layer as the AL333-28 medial cuneiform, was described as having a similar morphology. Contrastingly, in the OH8 foot, the first metatarsal OH8h, which articulates with the medial cuneiform OH8e, has a flat proximal articular surface and a similar morphology has been described for the first metatarsal SKX5017, which corresponds in size to the SKX31117 medial cuneiform (Susman, 1989).

<sup>2</sup>Re-examination of the SKX31117 medial cuneiform by one of the authors (TJ) indicates that this specimen does not represent a medial cuneiform and is probably non-hominin. Future investigation is needed to clarify this issue. The description used here follows Susman (1989).

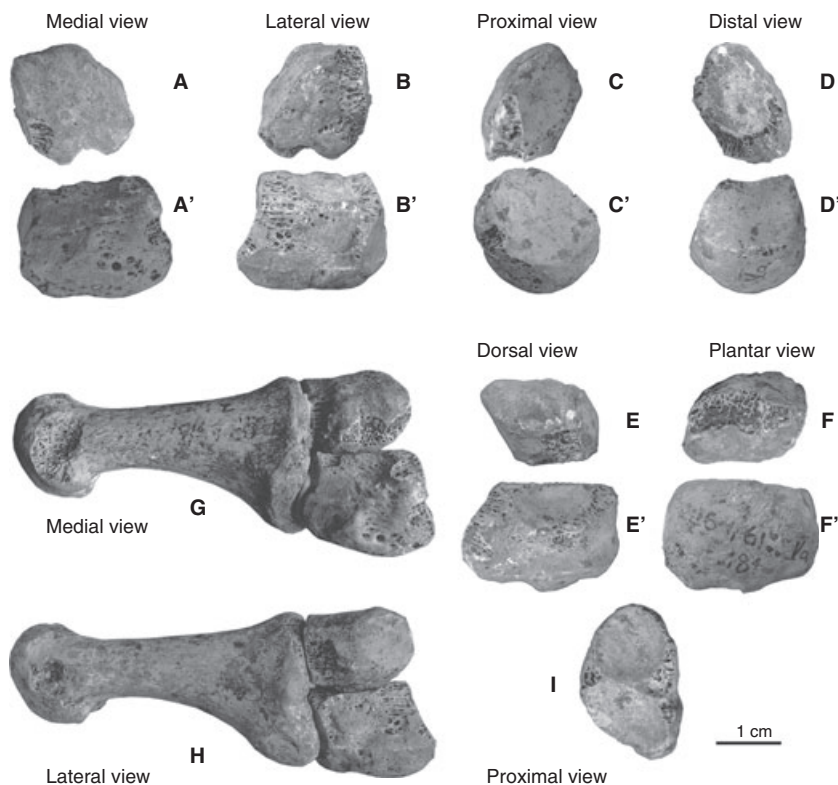


**Fig. 4** Dmanisi right medial cuneiform (D4111a/b) and first metatarsal (D3442). D4111a/b: (A–F) plantar part; (A'–F') dorsal part; (A,A') medial sides of plantar and dorsal parts, respectively; (B,B') lateral surfaces; (E,E') dorsal surfaces; (F,F') plantar surface; (C,C') proximal surface; (D,D') distal surface. D3442/D4111a/b in anatomical association: medial (G) and lateral (H) views. (I) D3442 proximal articular surface.

### The D4111a/b bipartite medial cuneiform and associated metatarsal D3442

D4111a/b is represented by a complete, undistorted and well-preserved pair of segments (Fig. 4). Post-mortem abrasions are present on surfaces of both segments. The plantar segment has only minor areas of abrasion on the lateral side (Fig. 4B'), which continue onto the articular surface of the dorsal part. The dorsal segment also has small abrasions on the lateral side, as well as on the articular surface for the base of the second metatarsal (Fig. 4B,F). The dorsal segment also exhibits a small amount of damage on the medial edge of its articular surface with the plantar segment (Fig. 4C).

The dorsal segment is relatively small and ovoid in shape (Fig. 4A–F), whereas the plantar segment is larger antero-posteriorly and cylindrical in shape (Fig. 4A'–F'). Articulation of the two segments creates a well-defined joint surface; the plantar surface of the dorsal segment is slightly convex (Fig. 4F), whereas the dorsal surface of the plantar segment is slightly concave (Fig. 4E'). The articulation between the two segments has a similarly smooth structure as the other articular surfaces on the bone, probably indicating the presence of a plane synovial joint covered by cartilage and synovial membrane.

The dorsal segment has a flattened articular surface for the base of the first metatarsal on its dorsal aspect, similar to what is reported in modern humans and the OH8e specimen (Fig. 4D). On the proximal side of the dorsal

segment, there is no articular surface for the navicular, as has been observed in cases of bipartite medial cuneiforms in modern humans (Barlow, 1942; Kjellström, 2004). Medial and lateral surfaces join each other at a ridge that demarcates the articular surface for the intermediate cuneiform and a roughened surface with well-defined tubercles for insertion of dorsal cuneonavicular ligaments proximally and the dorsal ligament of the first tarsometatarsal joint distally. The articular surface for the intermediate cuneiform is large and ovoid in form, and flattened with a dorso-plantar inclination on its lateral aspect (Fig. 4C). This form of articulation differs from the more narrow and elongated form that has been described in modern human samples, Stw573c and OH8e. The lateral side of the dorsal segment continues distally towards the articulation for the base of the second metatarsal (Fig. 4B). This surface, along with the articular surface for the intermediate cuneiform, forms a longitudinal ridge that is more closed-angled compared with modern humans and Stw573c/OH8e.

The plantar segment is divided distally by a longitudinal cleft forming a convexity on the articular surface for the base of the first metatarsal. Similar morphology is reported for the australopithecine specimens Stw573c and AL333-28 (Latimer et al. 1982; Clarke & Tobias, 1995); this morphology differs from the flat articular facet in modern humans and OH8e (Fig. 4D'). Although proximally the articular surface for the navicular is concave like in modern humans and Plio-Pleistocene hominins, it has an ovoid form that is elon-

gated dorso-medially to planto-laterally and facing laterally unlike in modern humans and Plio-Pleistocene hominins (Fig. 4C'). The medial surface of the plantar segment has a prominent tubercle for insertion of the tendon of *tibialis anterior* on its most anteroinferior angle (Fig. 4A'). The plantar surface of the plantar segment has a well-defined tubercle for the insertion of a slip of the tendon of *tibialis posterior* on its proximal side and, on its distal side, a tubercle for the insertion of the *peroneus longus* tendon (Fig. 4F').

The D3442 right first metatarsal (Fig. 4G–I) is large in dorso-plantar diameter compared with a typical modern human first metatarsal. It has a proximal articular surface divided into two facets by a horizontal ridge. The dorsal facet is mediolaterally concave, articulating with the anterior facet of the dorsal part of the medial cuneiform. The plantar facet is concave, articulating with the anterior convex facet of the plantar part of the medial cuneiform. Together, the two facets form an '8-shaped' articular contour, similar to the morphology reported for Stw753d and AL333-54. An '8-shaped' articular contour of the proximal first metatarsal has a low frequency in modern humans (2%) (Hartman & Mordret, 1889) and this condition is always associated with a medial cuneiform exhibiting some degree of bipartition (Barlow, 1942). This association also pertains to fossil hominin specimens D3443/D4111a/b and Stw573c/d.

### Morphometric analysis

All linear dimensions of the Dmanisi bipartite medial cuneiform fall below the corresponding mean values for the

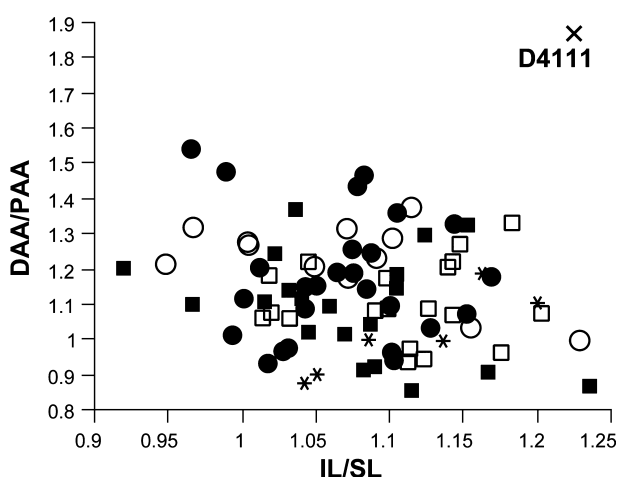


**Fig. 5** Medial cuneiform shape variation. Plot of ratio between distal and proximal articular surface areas [distal articular area (DAA) : proximal articular area (PAA)] vs. ratio between inferior and superior lengths (IL : SL). Black/white circles, Taforalt/Afalou; black/white squares, Laas/Afro-American; asterisks, Sigtuna bipartite medial cuneiforms; X, Dmanisi D4111.

modern human population samples analyzed here (Table 2). Most Dmanisi dimensions also fall below modern human ranges of variation. This is in agreement with the comparatively low body size estimates for this individual (Lordkipanidze et al. 2007).

The shape of the Dmanisi medial cuneiform can be characterized as follows: small proximal vs. distal articular surface; small superior vs. inferior length; and small overall length dimensions relative to breadth and height dimensions (Table 2 and Fig. 5). When comparing the Dmanisi medial cuneiform with that of bipartite or non-bipartite medial cuneiform of modern humans, three factors influencing patterns of shape variation have to be considered: (i) species-specific differences between Dmanisi and modern humans; (ii) size-related (allometric) differences; and (iii) differences between normal and bipartite medial cuneiforms.

Figure 5 shows that the bipartite cuneiform sample from Sigtuna is well within the mode of shape variation of human non-bipartite medial cuneiforms. Dmanisi is clearly separated from modern humans and differences in shape cannot be explained by differences in size alone. It is thus sensible to assume that differences between Dmanisi and the modern human sample do not reflect differences in the bipartite condition or allometric scaling but taxon-specific differences. The Dmanisi medial cuneiform is characterized by a relatively large inferior length and a relatively large distal articular surface, in congruence with the large base of metatarsal I.

### Discussion

#### Evolutionary developmental origins of the hominin foot and of medial cuneiform bipartition

Elements of the autopodium first appear in Devonian polydactylous tetrapods with six to eight digits (Coates & Clack, 1990). The pattern of basic tarsal units has undergone various evolutionary variations, including fusion or loss of elements and evolution of entirely new elements (Schaeffer, 1941). Because of the lack of evidence for successive fossil anatomy, it is difficult to infer homology within structures (Lewis, 1989). Differential fusion of the tarsal elements produces a wide spectrum of evolutionary developmental variation. In some species, separate cartilaginous precursors, which join during development to form one bone, bear evidence of phylogenetic history, whereas in other species, tarsal elements are highly derived and do not permit phylogenetic inferences (Lewis, 1989). Figure 6 shows the hypothetical basic tarsal units represented in human foot primordia; these include the talus (homologous to *os tibiale intermedium* and *os tibiale centrale proximale*), calcaneus (*os fibulare* and *os pisiforme*), navicular (*tibiale centrale distale* and *fibulare centrale distale*), tuberosity of the navicular (*os tibiale externum tarsi*), medial cuneiform (*os tarsale distale I* and distal end of the prehallux primordium),



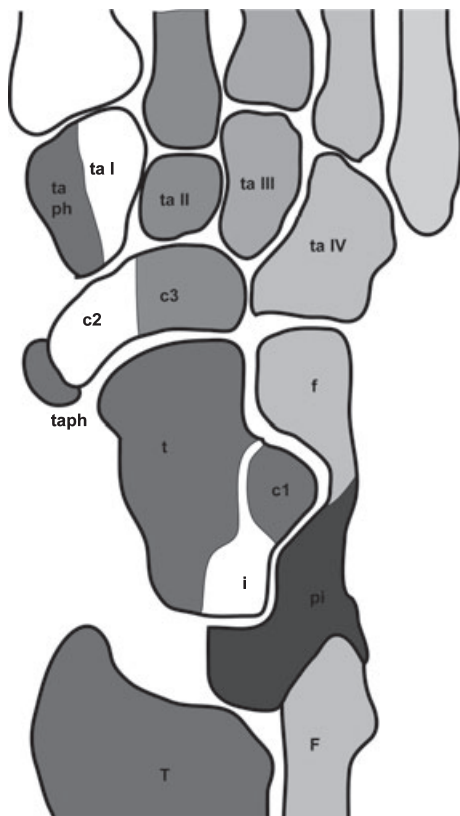


**Fig. 6** Homology of tarsal primordia in human. T, *tibia*; F, *fibula*; pi, *pisiforme*; i, *intermedium*; t, *tibiale*; f, *fibulare*; taph, *tarsalia praehallucis*; c1–3, *centralia*; ta I, *tarsale distale I*; ta II, *tarsale distale II*; ta III, *tarsale distale III*; ta IV, *tarsale distale IV* [redrawn after Čihák (1972)].

intermediate cuneiform (*os tarsale distale II*), lateral cuneiform (*os tarsale distale III*) and cuboid (*os tarsale distale IV*) (Čihák, 1972; Berman & Henrici, 2003).

Figures 7 and 8 give an overview of documented developmental pathways of the human medial cuneiform. Most frequently, it originates from a single mesenchymal primordium that ultimately develops into a single complete bone (Figs 7B and 8b1 → e1) (Scheuer & Black, 2000). In rare cases, a single complete medial cuneiform can arise from divided plantar and dorsal primordia that are separated by non-chondrified tissue (Figs 7A and 8b2 → e1) (Gardner et al. 1959; Čihák, 1972). The non-chondrified tissue constitutes a closely-packed mesenchymal-looking, cell-forming interzone (Pacifići et al. 2005) that eventually disappears and is replaced by other proliferating cells giving rise to a single complete bone (Fig. 8c1 → e1). Fusion of the two transient primordia (Figs 7A and 8b2 → c1) is interpreted as fusion of the *os tarsale distale I* and the prehallucial primordium (Čihák, 1972).

Bipartition can arise along two different developmental pathways (Barlow, 1942). Initial division in the mesenchymal primordium gives rise to a joint between two ossification centers (Figs 7A and 8b2 → c2), resulting in a bipartite med-

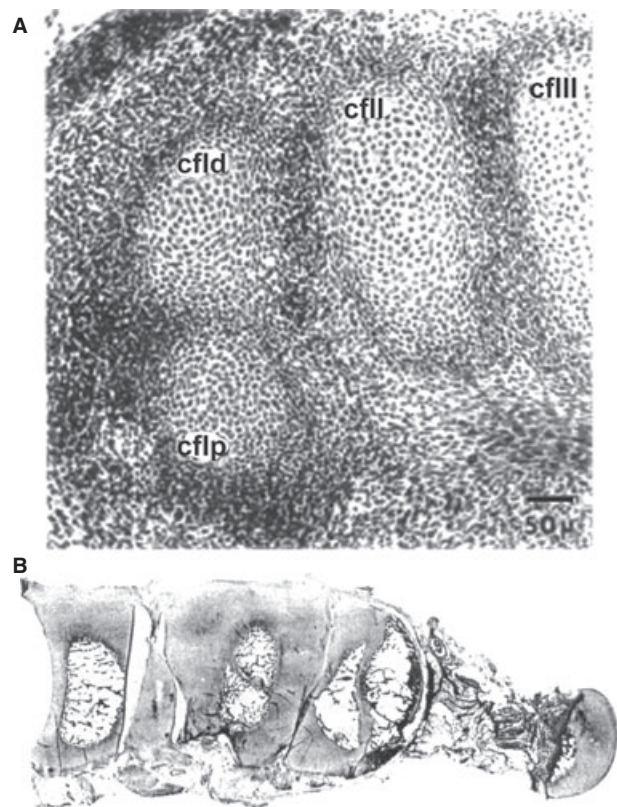
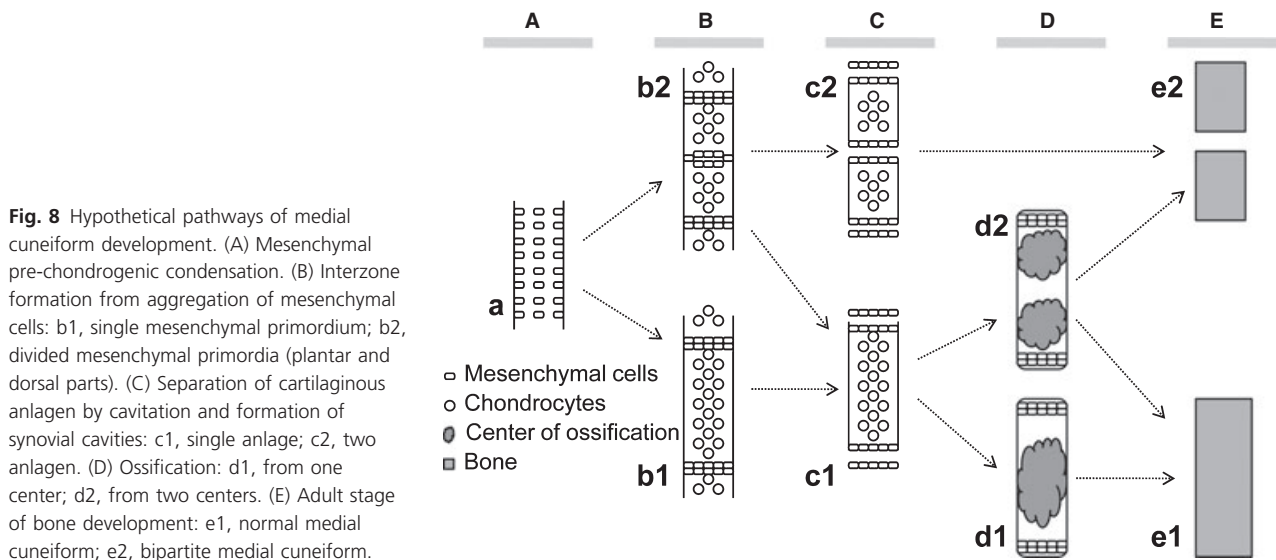


**Fig. 7** (A) Primordia of the bipartite dorsal (cflid) and plantar (cflp) medial, and intermedial (cflil) and lateral (cflil) cuneiform in a transverse section of the foot of a 19-mm embryo [from Čihák (1972). With kind permission of Springer Science+Business Media]. (B) Two ossification centers of a medial cuneiform. Copyright © 2010 by the American Orthopaedic Foot and Ankle Society, Inc., originally published in *Foot & Ankle International*, O'Neal et al. 1995 and reproduced here with permission.

ial cuneiform (Fig. 8c2 → e2) (Čihák, 1972). Alternatively, a single cartilaginous anlage gives rise to two ossification centers with a small fibrous cleft representing a hyaline synchondrosis (growth plate) between them (Figs 7B and 8c1 → d2), eventually resulting in two articulating bones (Fig. 8d2 → e2) (Pfitzner, 1896; O'Neal et al. 1995).

Genetic factors underlying variation in medial cuneiform developmental pathways might be identified at two different levels, namely Hox and Sox transcription factors, which specify the patterning and shape of the embryonic skeleton (Hall & Miyake, 2002; Cohen, 2006; Montero & Hurlé, 2007), or local regulators of mesenchymal condensation, which control the shape of the skeletal elements via auto-crane/paracrine factors (Garcia-Diego-Cazares et al. 2004; Hentschel et al. 2004; Pacifići et al. 2005; Cohen, 2006; Newman & Bhat, 2007). In the early stages of development, formation of a divided mesenchymal primordium (Fig. 8b2) could result from altered cell-intrinsic patterning at the gene level and/or variation in activator/inhibitor positional signaling mediators responsible for local control of the



mesenchymal primordium. In later stages of development, formation of two centers of ossification inside one single cartilaginous anlage (Fig. 8d2) could result from variation in activator/inhibitor positional signaling mediators responsible for local control of the cartilaginous anlage (Newman & Bhat, 2007). By the end of the adult stage of development, the outcome of both developmental scenarios would be a bipartite bone (Fig. 8e2), unless the separate bone precursors fuse producing a complete bone (Fig. 8e1).

Modern humans exhibit several variations in tarsal bone expression at low frequencies (Marti, 1947). These reflect homologous variants to the examples mentioned earlier: *os trigonum* (Zeichen et al. 1999; Chao, 2004; Mouhsine et al. 2004), *os perineum* (*cuboideum secundarium, centrale 4*) (Bloom, 1991), *os sustentaculi* (Bloom et al. 1986), *os naviculare bipartitum* (Cotta, 1961) and *os vesalianum* (Virchow, 1922; Lepore et al. 1990; Inoue et al. 1999; Boya et al. 2005). A supernumerary ossicle ('prehallux') situated at the disto-medial border of the medial cuneiform, or proximo-medial border of the first metatarsal, is common in Ceboidea and Hylobatidae. Such an ossicle also has been observed in pongids and *Homo* (Lewis, 1972; Wikander et al. 1986). The 'prehallux' may be a relict skeletal element of a pre-axial fin ray from the earliest phylogenetic stages of vertebrates (Lewis, 1972).

These non-random developmental variants provide the raw material on which selection has the potential to act during evolution (Alberch, 1983; Erlebacher et al. 1995). Morphological variants of the medial cuneiform also seem to result from a non-random pattern of developmental variation, i.e. different degrees of bipartition. Regarding the evolutionary developmental origins of bipartition, it may be speculated that the medial cuneiform is homologous to *os tarsale distale I* and the distal part of the prehallux primordium (Čihák, 1972; Berman & Henrici, 2003).

### Structure and function

In all clinical reports of a bipartite medial cuneiform, the condition was discovered incidentally during evaluation of subjects for a foot injury or a degenerative process in articular surfaces rather than an association with functional limitations of the foot (Dellacorte et al. 1992; O'Neal et al. 1995; Sener, 1999; Azurza & Sakellariou, 2001; Chiodo et al. 2002; Bismil et al. 2005; Fulwadhva & Parker, 2007). Presumably, the relatively flattened planar joint between the halves of the bipartite medial cuneiform does not restrict or alter motion of the medial ray of the foot.

In our modern human comparative sample, there was no indication that the bipartite medial cuneiforms of the Sigtuna sample significantly exceeded normal patterns of cuneiform shape variation. Morphological differences between the Dmanisi bipartite medial cuneiform and modern human cuneiforms thus most likely reflect species-specific differences, irrespective of whether these bones display bipartition. The articulation between the two segments of the Dmanisi medial cuneiform has a smooth structure, similar to the structure of other articular surfaces on these bones. This pattern is also apparent in articular surfaces of modern human bipartite medial cuneiforms. It is thus probable that the intracuneiform joint of Dmanisi, as in modern humans, was covered by cartilage and a synovial membrane.

Overall, it appears that the bipartite condition in the medial cuneiform represents developmental variation that does not cause significant overall morphological differences. Presumably the lack of morphological differences also implies a lack of functional differences. This provides an interesting perspective on the relationship of developmental and adaptive/functional constraints. The fact that the taxon-specific (most likely functionally relevant) morphology of the medial cuneiform can be reached by

different developmental pathways, some of which imply bipartition to various degrees, points toward higher-order, epigenetic constraints that canalize the development of midfoot morphology as a whole. This indicates morphogenetic homeostasis in the sense that foot ontogeny could be buffered against environmental noise as well as against developmental noise. Accordingly, it appears that the network of developmental pathways graphed in Fig. 8 not only gives rise to patterns of medial cuneiform variation but also provides the required developmental homeostasis, as developmental disturbance at any node or link in the network can be compensated by alternative pathways.

### Fossil hominin medial cuneiforms and first metatarsals

In hominoids, the distal articular surface of the medial cuneiform is convex, wide and medially-oriented, such that the articulating hallux is medially divergent. In humans this surface is flat, narrow and anteriorly-facing, such that the hallux does not diverge medially (Lewis, 1980, 1989). The latter condition exists in all described fossil hominin medial cuneiforms, which indicates that none of them are likely to have had a divergent hallux (McHenry & Jones, 2006). The Dmanisi bipartite medial cuneiform parallels this pattern.

In modern humans, morphology of the proximal joint surface of the first metatarsal (i.e. the surface articulating with the cuneiform) typically reflects the distal joint surface of the medial cuneiform. It is flat in the case of a single, non-bipartite medial cuneiform and it displays two facets separated by a transverse ridge ('8-shaped' circumference) in the case of a bipartite medial cuneiform. The latter association is observed in the relatively convex/concave first tarsometatarsal joint of the Dmanisi D3442/D4111a/b bones.

The situation is more complex in other Plio-Pleistocene hominins (Harcourt-Smith & Aiello, 2004; DeSilva, 2008; Proctor et al. 2008). The first tarsometatarsal joint surface is flat and undivided in OH8 and in SKX5017/SKX31117 (both attributed to *Homo*). In the Stw573 foot (attributed to *Australopithecus*), the proximal metatarsal surface has two facets. There is evidence that the same is true for the distal surface of the medial cuneiform. In the *A. afarensis* first metatarsal (AL333-54), the proximal articular surface exhibits two facets, whereas the only partially preserved medial cuneiform from the same stratigraphic location (AL333-28) bears no evidence of bipartition. However, not all first metatarsals attributed to *Australopithecus* reportedly exhibit a double facet (Day & Napier, 1964; Susman, 1989).

If we assume that a double-faceted proximal metatarsal joint surface is indicative of bipartition of the medial cuneiform in any of the three categories, it appears that this condition was relatively frequent in Plio-Pleistocene hominins compared with modern human populations. The

significance of a potentially higher incidence remains to be clarified. It could reflect increased developmental variation during evolutionary diversification of the hominin foot but it could also represent a sampling artifact.

### Conclusions

The Dmanisi D4111a/b bipartite medial cuneiform is the oldest known instance of this condition in the hominin fossil record. Incomplete bipartition in the form of a divided distal articular surface also appears in the medial cuneiform of the *A. africanus* foot Stw573, although this is not definite. In modern humans, bipartition has been reported to be rare and we find similarly low incidences (incomplete bipartition) in large samples of *Pan* and *Pongo*. Bipartition of the medial cuneiform is associated with a divided proximal articular surface of the first metatarsal in modern humans, in D3442/D4111a/b, and possibly in the Stw573 foot. Accordingly, the isolated *A. afarensis* metatarsal AL333-54, which exhibits a divided proximal surface, might also have been associated with a bipartite medial cuneiform. This raises the question whether this condition was more frequent in Plio-Pleistocene hominins than in extant humans and great apes.

In all linear dimensions, the Dmanisi bipartite medial cuneiform falls below the corresponding mean values for medial cuneiforms of modern human populations. In shape, the Dmanisi specimen differs significantly from modern human medial cuneiforms, indicating species-specific morphologies irrespective of the presence or absence of bipartition.

Various developmental pathways lead to bipartition or the normal condition of the medial cuneiform. Although these pathways generate developmental variation, the overall shape of the bone remains conserved. This indicates that the morphology of the medial cuneiform is constrained by higher-order processes of developmental integration. It is thus likely that bipartition is of no functional relevance.

### Acknowledgements

We would like to thank Kristian Carlson, Giorgi Berishvili and Massimo Delfino for suggestions and comments. We thank Anna Kjellström for granting access to the Sigtuna sample, Emmanuel Gilissen and Wim Wendelen for support during data collection in Tervuren, and Walther A. Fuchs for translation of 19<sup>th</sup> century German scientific texts. This work was supported by a Dan David 2003 scholarship, Wenner-Gren Foundation short-term fellowships, Swiss National Science Foundation grants 3100A0-109344/1 and IZ7330-110895, and Georgian National Science Foundation grant GNSF/ST 06/5-048.

### References

- Alberch P (1983) Morphological variation in the neotropical salamander genus *Bolitoglossa*. *Evolution* **37**, 906–919.

- Azurza K, Sakellariou A (2001) "Osteosynthesis" of a symptomatic bipartite medial cuneiform. *Foot Ankle Int* **22**, 499–501.
- Barclay M (1932) A case of duplication of the internal cuneiform bone of the foot (*Cuneiforme Bipartitum*). *J Anat* **67**, 175–177.
- Barlow TE (1942) Os cuneiforme 1 bipartitum. *Am J Phys Anthropol* **29**, 95–111.
- Berman DS, Henrici AC (2003) Homology of the astragalus and structure and function of the tarsus of Diadectidae. *J Paleontol* **77**, 172–188.
- Bismil Q, Foster PAL, Venkateswaran B, et al. (2005) Symptomatic bipartite medial cuneiform after injury: a case report. *J Foot Ankle Surg* **11**, 55–58.
- Bloom RA (1991) The infracalcaneal os peroneum. *Acta Anat (Basel)* **140**, 34–36.
- Bloom RA, Libson E, Lax E, et al. (1986) The assimilated os sustentaculi. *Skel Radiol* **15**, 455–457.
- Böker H, Müller W (1936) [The os cuneiforme 1 bipartitum, a progressive developmental stage of the transverse arch of the human foot.] *Anat Anz* **83**, 193–204.
- Boya H, Ozcan O, Tandogan R, et al. (2005) Os vesalianum pedis. *J Am Podiatr Med Assoc* **95**, 583–585.
- Chao W (2004) Os trigonum. *Foot Ankle Clin* **9**, 787–796.
- Chiodo CP, Parentis MA, Myerson MS (2002) Symptomatic bipartite medial cuneiform in an adult athlete: a case report. *Foot Ankle Int* **23**, 348–351.
- Čihák R (1972) Ontogenesis of the skeleton and intrinsic muscles of the human hand and foot. *Adv Anat Embryol Cell Biol* **46**, 7–177.
- Clarke RJ, Tobias PV (1995) Sterkfontein Member 2 foot bones of the oldest South African hominid. *Science* **269**, 521–524.
- Coates MI, Clack JA (1990) Polydactyly in the earliest known tetrapod limbs. *Nature* **347**, 66–69.
- Cohen MM Jr (2006) The new bone biology: pathologic, molecular, and clinical correlates. *Am J Med Genet A* **140**, 2646–2706.
- Cotta H (1961) Ein Beitrag zur Differentialdiagnose der Navicularpseudarthrose – *Os naviculare bipartitum carpi*. *Arch Orthop Unfallchir* **52**, 581–589.
- Day MH, Napier JR (1964) Hominid fossils from Bed I, Olduvai Gorge, Tanganyika: fossil foot bones. *Nature* **201**, 969–970.
- Dellacorte MP, Lin PJ, Grisafi PJ (1992) Bilateral bipartite medial cuneiform: a case report. *J Am Podiatr Med Assoc* **82**, 475–478.
- Deloison Y (2004) A new hypothesis on the origin of hominoid locomotion. In *From Biped to Strider: The Emergence of Modern Human Walking, Running, and Resource Transport* (eds Meldrum DJ, Hilton CE), pp. 35–47. New York: Academic/Plenum Publishers.
- DeSilva JM (2008) Vertical Climbing Adaptations in the Anthropoid Ankle and Midfoot: Implications for Locomotion in Miocene Catarrhines and Plio-Pleistocene Hominins. PhD Dissertation. p. 381. Michigan: The University of Michigan.
- Eggimann P (1951) [Bipartition of the semilunar bone.] *Radiol Clin* **20**, 65–70.
- Elias I, Dheer S, Zoga AC, et al. (2008) Magnetic resonance imaging findings in bipartite medial cuneiform – a potential pitfall in diagnosis of midfoot injuries: a case series. *J Med Case Rep* **2**, 272.
- Erlebacher A, Filvaroff EH, Gitelman SE, et al. (1995) Toward a molecular understanding of skeletal development. *Cell* **80**, 371–378.
- Friedlowsky A (1870) Über Vermehrung der Handwurzelknochen durch ein Os carpale intermedium und über secundäre Fußwurzelknochen. [On the multiplication of carpal bones through an os carpale intermedium, and on secondary tarsal bones.] *Sitzungsber Akad Wissensch* **LXI**, 582–596.
- Fulwadhva U, Parker RJ (2007) Symptomatic bipartite medial cuneiform. *Appl Radiol* **3**, 42–44.
- Garcia-Cardenas D, Rosales C, Katoh M, et al. (2004) Coordination of chondrocyte differentiation and joint formation by  $\alpha 5\beta 1$  integrin in the developing appendicular skeleton. *Development* **131**, 4735–4742.
- Gardner E, O'Rahilly R, Gray DJ (1959) The prenatal development of the skeleton and the joints of the human foot. *J Bone Joint Surg Am* **41**, 847–851.
- Gruber W (1877) Ueber das *Os cuneiforme I. bipartitum* und seine secundären Stücke: *Os cuneiforme I secundarium dorsale* und *Os cuneiforme I. secundarium plantare*. *Mém Acad Sci St Pétersbourg* **VII**, 5–31.
- Gruber W (1883) *Os lunatum carpi* mit einem Anhang am dorsalen Ende. *Lunatum bipartitum*. *Virchows Arch* **94**, 349–353.
- Gruber W (1884) Drei neue Fälle von *Os lunatum carpi bipartitum* und ein Fall von *Os lunatum tripartitum* (vorher nicht gesehen) – Verhalten des *Os lunatum secundarium dorsale* wie ein "Os centrale carpi medium" in einem veröffentlichten Falle und in neuen Fällen. *Virchows Arch* **98**, 408–413.
- Hall KB, Miyake T (2002) All for one and one for all: condensations and the initiation of skeletal development. *Bioessays* **22**, 138–147.
- Harcourt-Smith WEH, Aiello LC (2004) Fossils, feet and the evolution of human bipedal locomotion. *J Anat* **204**, 403–416.
- Hartman H, Mordret J (1889) Sur un point de l'anatomie du premier cunéiforme. *Bull Soc Anat Paris, Ser V* **3**, 71–82.
- Hentschel HGE, Glimm T, Glazier JA, et al. (2004) Dynamical mechanisms for skeletal pattern formation in the vertebrate limb. *Proc R Soc Lond B* **271**, 1713–1722.
- Hubner A (1953) [Bipartition of navicular bone of the wrist.] *Monatsschr Unfallheilkd Versicherungsmed* **56**, 193–195.
- Inoue T, Yoshimura I, Ogata K, et al. (1999) *Os vesalianum* as a cause of lateral foot pain: a familial case and its treatment. *J Pediatr Orthop B* **8**, 56–58.
- Jungers WL, Harcourt-Smith WEH, Wunderlich RE, et al. (2009) The foot of *Homo floresiensis*. *Nature* **459**, 81–84.
- Kjellström A (2004) A case study of *os cuneiforme mediale bipartitum* from Sigtuna, Sweden. *Int J Osteoarchaeol* **14**, 475–480.
- Latimer BM, Lovejoy CO, Johanson DC, et al. (1982) Hominid tarsal, metatarsal, and phalangeal bones recovered from the Hadar formation: 1974–1977 collections. *Am J Phys Anthropol* **57**, 701–719.
- Lepore L, Pagliuca S, Francobandiera C (1990) Os tibiale externum: etiopathogenesis, cases, clinical aspect and treatment. *Chir Organi Mov* **75**, 307–310.
- Lewis OJ (1972) The evolution of the hallucial tarsometatarsal joint in the anthropoidea. *Am J Phys Anthropol* **37**, 13–33.
- Lewis OJ (1980) The joints of the evolving foot. Part III. The fossil evidence. *J Anat* **131**, 275–298.
- Lewis OJ (1989) *Functional Morphology of the Evolving Hand and Foot*. Oxford: Clarendon Press.
- Lordkipanidze D, Vekua A, Ferring R, et al. (2005) The earliest toothless hominin skull. *Nature* **434**, 717–718.



- Lordkipanidze D, Vekua V, Ferring R, et al. (2006) A fourth hominin skull from Dmanisi, Georgia. *Anat Rec* **288A**, 1146–1157.
- Lordkipanidze D, Jashashvili T, Vekua A, et al. (2007) Postcranial evidence from early *Homo* from Dmanisi, Georgia. *Nature* **449**, 305–310.
- Lovejoy CO, Latimer B, Suwa G, et al. (2009) Combining prehension and propulsion: the foot of *Ardipithecus ramidus*. *Science* **326**, 72e1–72e8.
- Mariotti V, Bonfiglioli B, Facchini F, et al. (2009) Funerary practices of the Iberomaurusian population of Taforalt (Tafoughalt; Morocco, 11–12,000 BP): new hypotheses based on a grave by grave skeletal inventory and evidence of deliberate human modification of the remains. *J Hum Evol* **56**, 340–354.
- Marti T (1947) Die Skelettvarietäten des Fusses, ihre klinische und unfallmedizinische Bedeutung. [Skeletal variants of the foot; their clinical and traumatological significance.] *Prakt Beitr Orthop* **58**, 1–164.
- Martin R, Saller K (1957) *Lehrbuch der Anthropologie in systematischer Darstellung mit besonderer Berücksichtigung der anthropologischen Methoden* (3rd edn). Stuttgart: Fischer.
- Mau H (1960) Zur Kenntnis des Naviculare bipartitum pedis. [Contribution to the knowledge of the bipartite navicular bone of the foot.] *Z Orthop Grenzgeb* **93**, 404–410.
- McHenry HM, Jones AL (2006) Hallucial convergence in early hominids. *J Hum Evol* **50**, 534–539.
- Mirazón Lahr M, Arensburg B (1995) Skeletal robusticity in the Epipaleolithic of North Africa and the Levant. *Paléorient* **21**, 87–96.
- Montero AJ, Hurlé MJ (2007) Deconstruction digit chondrogenesis. *Bioessays* **29**, 725–737.
- Mouhsine E, Djahangiri A, Garofalo R (2004) Fracture of the non fused os trigonum, a rare cause of hindfoot pain. A case report and review of the literature. *Chir Organi Mov* **89**, 171–175.
- Newman SA, Bhat R (2007) Activator-inhibitor dynamics of vertebrate limb pattern formation. *Birth Defects Res C* **81**, 305–319.
- O'Neal ML, Ganey TM, Ogden JA (1995) Fracture of a bipartite medial cuneiform synchondrosis. Bilateral bipartite medial cuneiform. A case report. *Foot Ankle Int* **16**, 37–40.
- Pacifici M, Koyama E, Iwamoto M (2005) Mechanisms of synovial joint and articular cartilage formation: recent advances, but many lingering mysteries. *Birth Defects Res C* **75**, 237–248.
- Pfützner W (1896) Beiträge zur Kenntniss des menschlichen Extremitätenskelets. [Contributions to the knowledge of the human limb skeleton.] *Morphol Arbeiten* **6**, 245–528.
- Proctor DJ, Broadfield D, Proctor K (2008) Quantitative three-dimensional shape analysis of the proximal hallucial metatarsal articular surface in *Homo*, *Pan*, *Gorilla*, and *Hylobates*. *Am J Phys Anthropol* **135**, 216–224.
- Randelli M (1961) [On bipartition of the carpal scaphoid.] *Arch Ortop* **74**, 700–706.
- Richards RR, Ledbetter WS, Transfeldt EE (1987) Radiocarpal osteoarthritis associated with bilateral bipartite carpal scaphoid bones: a case report. *Can J Surg* **30**, 289–291.
- Schaeffer B (1941) The morphological and functional evolution of the tarsus in Amphibians and Reptiles. *Bull Am Mus Nat Hist* **78**, 396–472.
- Scheuer L, Black S (2000) *Developmental Juvenile Osteology*. London: Academic Press.
- Schmitt E, Schmitt O (1983) [Bipartite lunate bone.] *Z Orthop Ihre Grenzgeb* **121**, 192–195.
- Sener RN (1999) Bilateral extra tarsal bones in Rubinstein–Taybi syndrome: the fourth cuneiform bones. *Eur Radiol* **9**, 483–484.
- Shawdon A, Kiss Z, Fuller P (1995) The bipartite tarsal navicular bone: radiographic and computed tomography findings. *Austral Radiol* **39**, 192–194.
- Smith T (1866) A foot having four cuneiforms. *Trans Pathol Soc Lond* **17**, 222–223.
- Susman RL (1989) New hominid fossils from the Swartkrans formation (1979–1986 excavations): postcranial specimens. *Am J Phys Anthropol* **79**, 451–474.
- Trinkaus E (1983) *The Shanidar Neandertals*. New York: Academic Press.
- Turner WM (1869) Report on the progress of anatomy. *J Anat Physiol* **3**, 447–459.
- Vekua A, Lordkipanidze D, Rightmire GP, et al. (2002) A new skull of early *Homo* from Dmanisi, Georgia. *Science* **297**, 85–89.
- Virchow H (1922) Das vorn und hinten gefurchte erste Keilbein am Fusse des Menschen. [The anteriorly and posteriorly grooved first cuneiform of the human foot.] *Anat Anz* **24–27**, 79–86.
- Volk C (1937) Zwei Fälle von *os naviculare pedis bipartitum*. [Two cases of bipartite navicular bone of the foot.] *Z Orthop* **66**, 396–403.
- Volkov T (1904) Variations squelettiques du pied. [Skeletal variations of the foot.] *Bull Soc Anat Paris, Ser V* **5**, 1–331.
- Weber H-J (1956) Metatarsus adductus congenitus duplex bei *Os cuneiforme I bipartitum*. *Arch Orthop Unfall-Chir* **48**, 399–402.
- Wikander R, Covert HH, DeBlieux DD (1986) Ontogenetic, intraspecific, and interspecific variation of the prehallux in primates: implications for its utility in the assessment of phylogeny. *Am J Phys Anthropol* **70**, 513–523.
- Wiley JJ, Brown DE (1981) The bipartite tarsal scaphoid. *J Bone Joint Surg* **63-B**, 583–586.
- Willich CT (1925) Metatarsus adductus congenitus duplex mit Malazie am *Os cuneiforme I. bipartitum*. [Metatarsus adductus congenitus duplex with pathology of the *Os cuneiforme I. bipartitum*.] *Arch Orthop Traum Su* **23**, 576.
- Zeichen J, Schrott E, Bosch U, et al. (1999) [Os trigonum syndrome.] *Unfallchirurg* **102**, 320–323.
- Zimmer EA (1938) Krankheiten, Verletzungen und Varietäten des *Os naviculare pedis*. *Arch Orthop Unfallchir* **38**, 396–411.